

Proton periphery activated by multiparticle dynamics

I.M. Dremin^a, V.A. Nechitailo^{a,b}

^a*P.N. Lebedev Physical Institute, Moscow 119991, Russia*

^b*Institute of Theoretical and Experimental Physics, Moscow, Russia*

Abstract

It is shown that protons become more active at the periphery with increase of their collision energy. By computing the impact parameter distribution of the proton-proton overlap function at LHC energies and comparing it with ISR (and $Spp\bar{p}S$ for $p\bar{p}$) data, we conclude that the peripheral region of protons plays an increasing role in the rise of total cross sections through multiparticle dynamics. The size of the proton as well as its blackness increase with energy. The protons become more black both in the central region and, especially, at the periphery. This effect can be related to the ridge phenomenon and to the inelastic diffraction processes at LHC energies.

Keywords: elastic scattering, proton, overlap function

It is well known that parton (quark, gluon) densities and the share of low- x partons rise with increasing energies of colliding hadrons. Less attention has been paid to the analysis of the spatial distribution of the parton content inside them and its evolution with energy. This can be done by studying the structure of the overlap function in the unitarity condition for the elastic scattering amplitude in the impact parameter representation at different energies of colliding protons. The very first analyses [15, 14, 2] have led to extremely interesting conclusions about the increasing peripherality of protons within the rather narrow interval of ISR energies. Later, this was confirmed and strengthened at somewhat higher energies by the $Spp\bar{p}S$ data [1]. It was shown that while the increase of the overlap function at the proton periphery is quite modest in the ISR energy range (about 4%), it becomes much stronger (about 12%) if $Spp\bar{p}S$ energies are included. However, no sizeable change of the proton blackness was noticed at small distances in this energy interval. The similar effect at HERA energies was discussed in [19] for the vector meson production process in the framework of the dipole-proton scattering model.

That is why we attempt to learn if peripheral regions of protons become even more active at LHC energies and the central region is activated as well. The striking, but not at all unexpected, result is that this increase persists and extends to smaller impact parameters now. It amounts to about 40% of edge corrections at distances about 1 fm. The main parton content in the overall region of inelastic collisions remains relatively constant and below the unitarity bound in the central region of impact parameters less than about 0.5 fm but also indicates some increase of opacity compared to lower energies.

We proceed by using the approach adopted in [2]. First of all, the TOTEM data on the differential cross section of elastic pp -scattering at 7 TeV [4] are fitted by the formula (1) for the elastic scattering amplitude $f(s, t)$ (which depends on the center-of-mass energy \sqrt{s} and the transferred

Email address: dremin@lpi.ru (I.M. Dremin)

momentum $\sqrt{|t|}$ proposed in [20]:

$$f(s, t) = i\alpha[A_1 \exp(\frac{1}{2}b_1\alpha t) + A_2 \exp(\frac{1}{2}b_2\alpha t)] - iA_3 \exp(\frac{1}{2}b_3 t), \quad (1)$$

where $\alpha(s)$ is complex and is given by

$$\alpha(s) = [\sigma_{tot}(s)/\sigma_{tot}(23.5 \text{ GeV})](1 - i\rho_0(s)). \quad (2)$$

Even though this parametrization has no theoretical foundation, it provides in a wide energy interval good phenomenological fits of differential cross sections¹ defined as

$$\frac{d\sigma}{dt} = |f(s, t)|^2. \quad (3)$$

The normalization at the optical point is

$$\sigma_{tot}(s) = \sqrt{16\pi} \text{Im} f(s, 0). \quad (4)$$

We shall also use the ratio of the real to imaginary parts of the amplitude

$$\rho(s, t) = \frac{\text{Re} f(s, t)}{\text{Im} f(s, t)}. \quad (5)$$

The following values of the parameters have been fixed by the fit to the experimental points of the differential cross section at the energy 7 TeV in the range $0.0052 < |t| < 2.44 \text{ GeV}^2$:

$$\begin{aligned} A_1^2 &= 55.09 \text{ mb/GeV}^2, & A_2^2 &= 3.46 \text{ mb/GeV}^2, & A_3^2 &= 1.47 \text{ mb/GeV}^2, \\ b_1 &= 8.31 \text{ GeV}^{-2}, & b_2 &= 4.58 \text{ GeV}^{-2}, & b_3 &= 4.70 \text{ GeV}^{-2}. \end{aligned} \quad (6)$$

We have also used $\sigma_{tot}(7 \text{ TeV}) = 98.58 \text{ mb}$ and $\rho_0(7 \text{ TeV}) = 0.14$ which leads to $\rho(s, 0) = 0.148$. The parameter ρ_0 defines $\rho(s, 0)$ but not coincides with it. The normalization of $|f(s, t)|^2$ in mb/GeV^2 allows direct comparison with [2]. Note that the exponentials in first two terms are determined by the product of b_i and $\alpha(s)$.

The good quality of the fit with these values is seen in Fig. 1. A complete error analysis would lie beyond the scope of this paper. We have just estimated that uncertainties are small by varying the measured quantities inside the $\pm 1\sigma$ error bars. Thus, we consider the formula (1) as an empirical insert suitable for the numerical fit of experimental data and use it in further calculations. The fit is almost insensitive to the parameter ρ_0 except of the dip region. With some adjustment of parameters A_i, b_i , the fit is also satisfactory if one adopts the value of $\rho(s, 0) = 0.107$ favored by the recent results of the TOTEM collaboration [21].

One is able to compute from (1) the real and imaginary parts of the amplitude at any value of the transferred momentum t using these parameters. They are shown in Fig. 2. Each of them has a single zero. The evolution of their ratio $\rho(s, t)$ with the transferred momentum t is mainly prescribed by the last term in this formula with the negative sign in front of it and small exponential b_3 . The ratio $\rho(s, t)$ for $\sqrt{s}=7 \text{ TeV}$ is also shown in Fig. 2. It clearly demonstrates that

¹There are many others (albeit with larger number of adjustable and hidden parameters) reviewed in [10] and recently published [6, 12, 17, 18].

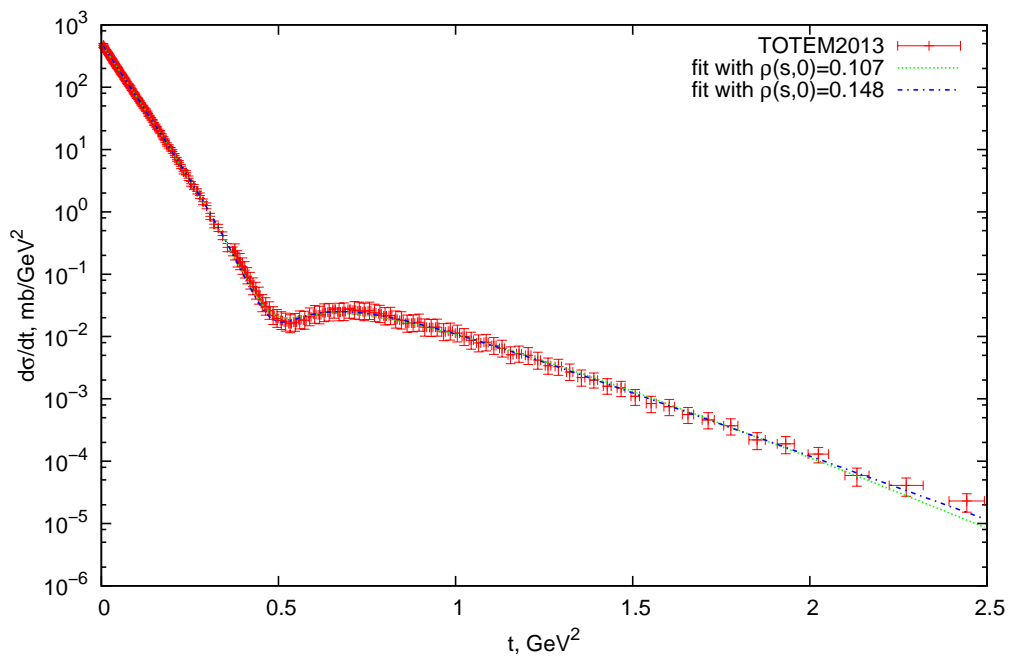


Figure 1: Fit of the TOTEM data – dotted and dash-dotted curves. Dotted curve is calculated with parameter $\rho(s,0) = 0.107$ and dash-dotted curve with $\rho(s,0) = 0.148$

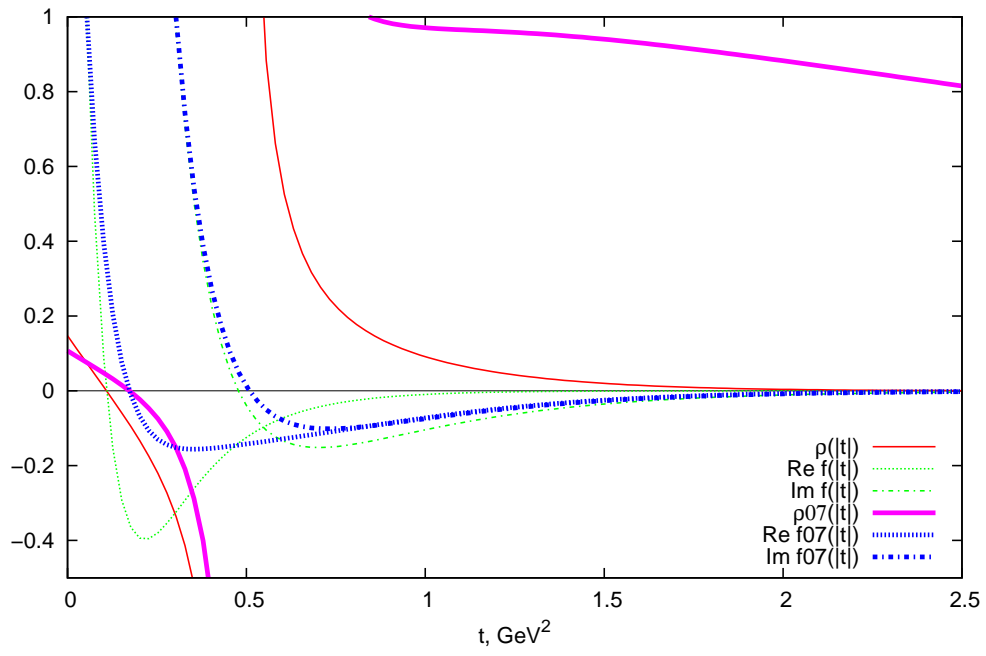


Figure 2: Real (dotted curve) and imaginary (dash-dotted curve) parts of the amplitude and their ratio (solid curve). Bold lines are for $\rho(s, 0) = 0.107$.

the real part is small and can be neglected everywhere except near the point where the imaginary part is equal to zero.

The new feature seen in Fig. 2 is the difference in values of $\rho(s, t)$ in the Orear region for the two choices of $\rho(s, 0)$. It becomes of the order of 1 for $\rho(s, 0) = 0.107$. Note that in both cases it strongly differs from its average value about -2 required by the fit according to the solution of the unitarity equation [11]. The solution [3] predicts the exponential of $\sqrt{|t|}$ -behavior of the amplitude. It poses an interesting problem which has not yet been resolved.

This ratio can change the sign if more zeros of either imaginary or real parts of the amplitude appear. For example, this happens in the model of [17]. It incorporates phenomenologically the Orear type behavior of the amplitude at larger transferred momenta (albeit in a way somewhat different from [3]) and predicts two zeros of the real part. Then, the ratio reaches large negative values at high transferred momenta. It can solve the above puzzle. The somewhat smaller absolute values at large $|t|$ are also predicted in the model using the inverse of polynomials [6] as described in [17]. The analysis of [17] clearly shows that the somewhat modified description of the amplitude at larger transferred momenta can change our conclusions about the behavior of this ratio there.

To reveal the space structure of proton interactions, the amplitude $f(s, t)$ must be rewritten in the impact parameter space in place of the momentum space. By applying the Fourier-Bessel transformation, we define the dimensionless profile function

$$i\Gamma(s, b) = \frac{1}{\sqrt{\pi}} \int_0^\infty dq q f(s, t) J_0(qb). \quad (7)$$

Here, the variable b , called the impact parameter, describes the vector joining the centers of colliding protons at the moment of their collision, $q = \sqrt{-t}$, and J_0 is the Bessel function of zero order.

The amplitude $f(s, t)$ must satisfy the unitarity condition. For $t = 0$, it states that the total cross section is a sum of cross sections of elastic and inelastic processes. If written in the impact parameter representation (7) it looks like

$$2\text{Re} \Gamma(s, b) = |\Gamma(s, b)|^2 + G(s, b), \quad (8)$$

where G is called the overlap function in the impact parameter space.

The smallness of the real part of $f(t)$ corresponding to small $\text{Im} \Gamma(s, b)$ implies that one can compute G approximately as

$$G(s, b) \approx 2\text{Re} \Gamma(s, b) - (\text{Re} \Gamma(s, b))^2. \quad (9)$$

The physics meaning of these relations is very simple. The overlap function G describes the kinematical overlap of two cones filled in by the inelastically produced secondary particles in the momentum space expressed in terms of the proton structure at a given impact parameter b . In other words, it corresponds to the particle distribution $d^2\sigma/d\mathbf{b}$ in the impact parameter space. One may treat it as a parton distribution if one-to-one correspondence of particles and partons is assumed.

The overlap function at 7 TeV has a form shown in Fig. 3 by the upper dash-dotted curve. Its dependence on $\rho(s, 0)$ is so weak that can be neglected. However, as we see, it strongly differs from the corresponding function at ISR energy 23.5 GeV (shown by the lower solid curve), especially at the very edge of the distribution. The overlap function at 7 TeV declines steeply

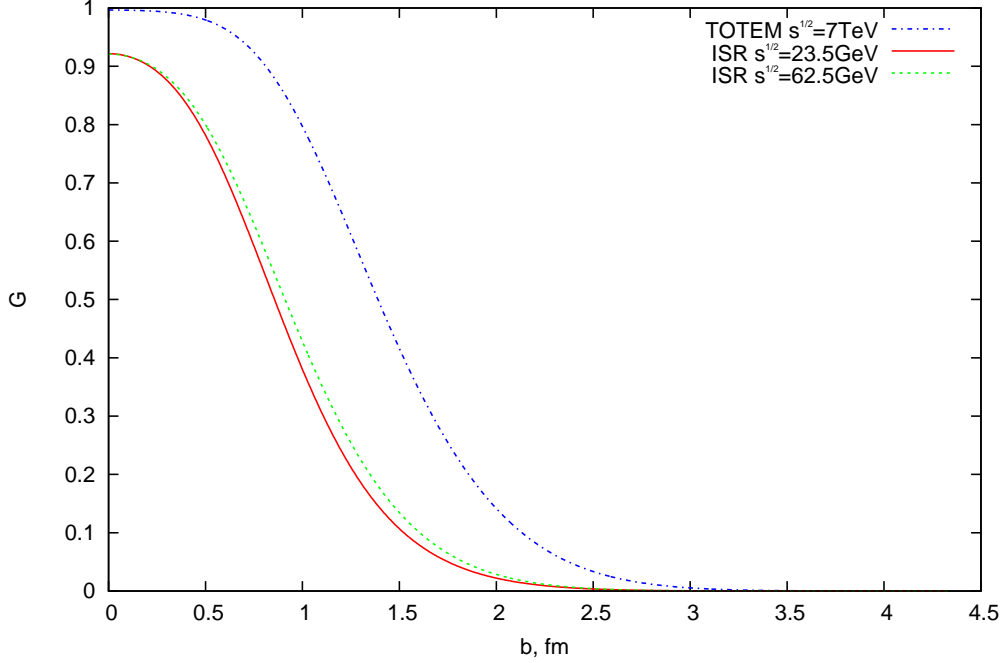


Figure 3: The overlap functions at 23.5 GeV (solid curve), 62.5 GeV (dotted curve) and 7 TeV (dash-dotted curve)

but there is no sharp cutoff at large impact parameters. At $b = 0$, it approaches the unitarity limit corresponding to the complete blackness. This is a clear manifestation of the parton saturation effect.

The difference between the two functions $\Delta G(b) = G(s_1, b) - G(s_2, b)$ ($\sqrt{s_1} = 7 \text{ TeV}$, $\sqrt{s_2} = 23.5 \text{ GeV}$) results because of the increase of the elastic cross section and shrinkage of the diffraction cone with energy. In other words, it demonstrates the increase of the opacity since the ratio σ_{el}/σ_{tot} increases also, and it is proportional to the opacity.

In Fig. 4, we demonstrate the difference between these two distributions (the upper curve). It is mainly concentrated at the periphery of the proton at the distance about 1 fm. This feature is stable against the variations of $\rho(s, 0)$. It shows that, at higher energies, the peripheral region becomes more populated by partons, and they play more active role in particle production.

It is tempting to ascribe the peripheral nature of this effect to two features of inelastic processes observed already at LHC. First, the collisions with impact parameters about 1 fm lead to the almond-shaped overlap region. Therefore, due to increase of the parton density they become responsible for the ridge-effect visible in high multiplicity pp-processes at LHC but not observed at lower energies. Second, the more peripheral collisions with larger impact parameters would lead to strong increase of the cross section of the inelastic diffraction with large masses and high multiplicities which can hardly be separated by the gap criteria from the minimum bias events. This is especially interesting because the cross section of the low-mass diffraction is rather small at 7 TeV [5] and surprisingly close to its values at ISR energies. The stronger absorption in the peripheral region at 7 TeV results in the suppression of the low-mass inelastic diffraction processes. It looks as if it is necessary to include the states of the continuum spectrum beside the

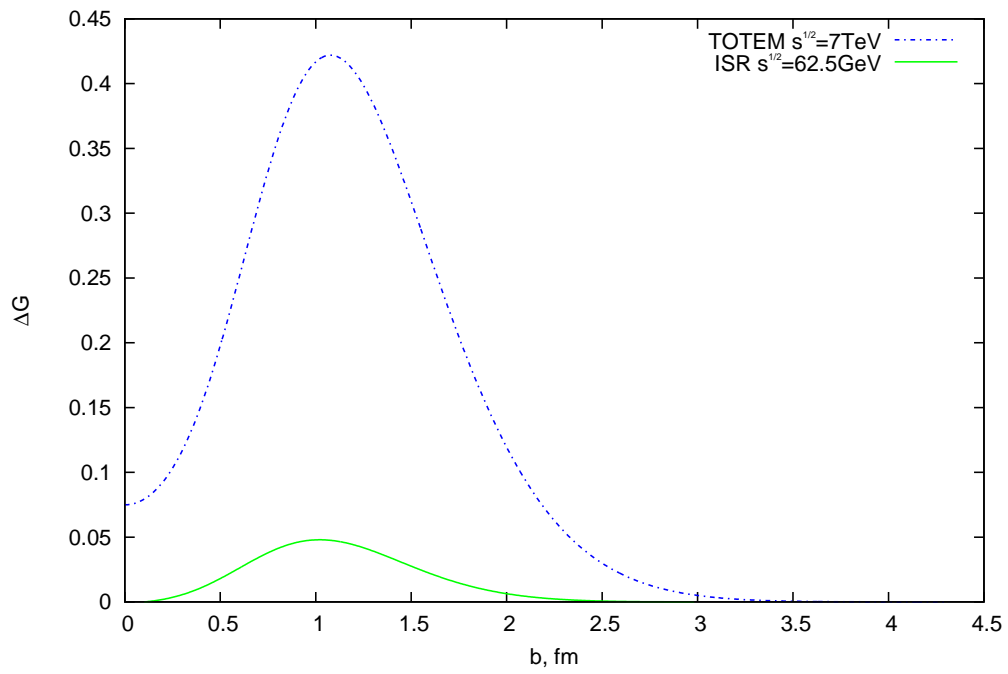


Figure 4: The difference between the overlap functions. Dash-dotted curve is for 7 TeV and 23.5 GeV energies, solid curve is for 62.5 GeV and 23.5 GeV energies

discrete bare eigenstates in the traditional approach [13].

We note that the Regge-type models of inelastic diffraction [16] do not agree with the observed decrease below 1 at 7 TeV of the parameter $Z = 4\pi B/\sigma_{tot}$ studied in [10] because they predict that this parameter is equal to $1 + \sigma_{in}^D/\sigma_{el}$ greater than 1 (where σ_{in}^D is the cross section of the low-mass inelastic diffraction). It has been pointed out in [3] that this parameter defines the slope of $d\sigma/dt$ beyond the diffraction cone in the Orear region. Its further decrease with energy would result [8] in first signatures of the approach to the black disk limit to appear just in there.

Another new feature, seen in Fig. 4, is the quite large (about 0.08) value of $\Delta G(b)$ at small impact parameters that reveals a stronger blackness of the disk at higher energies and is related to the rise of the cross section of the main bulk of inelastic processes. No signs of this effect have been found at lower energies. These observations are tightly related to the visible violation of geometric scaling even in the diffraction cone at LHC energies [9] because of the dual correspondence of the transferred momenta t and the impact parameters b . Probably, they correspond also to disagreement between experimental data at 7 TeV and predictions of Monte Carlo models seen in high multiplicity events [7].

In the same Figure, the lower curve corresponds to the similar (albeit much smaller!) difference $\Delta G(b)$ within the quite narrow ISR energy interval (23.5 - 62.5 GeV). It was stressed in [2] that this difference is negligibly small at low impact parameters while showing some statistically significant excess about 4% at the periphery².

We stress that the formula (1) has been applied just for analytic approximation of experimental data with the smallest number of adjustable parameters. Its extrapolation to the yet unmeasured regions of $d\sigma/dt$ can hardly change the main conclusion qualitatively. The range of $|t|$ below 0.005 GeV^2 ($p_T < 70 \text{ MeV}$; large b) is well fitted by the normalization to the optical point. In the range of $|t| > 2.5 \text{ GeV}^2$, the values of $d\sigma/dt$ become extremely small to seriously influence the qualitative conclusions about the energy evolution of the spatial picture described above. However, we should point out that the behavior at larger transferred momenta is important for understanding the relative role of real and imaginary parts and can somewhat change the quantitative estimates of ΔG . Also, the slight variations of the overlap function at low b are crucial for theoretical modelling.

Comparison of the curves in Fig. 4 leads to the conclusion that the size of the proton as well as its blackness increase with energy. The protons become more black both in the central region, where they almost reach the saturation of the unitarity condition, and, especially, at the periphery, where the parton density strongly increases. Multiparticle dynamics is in charge of these effects.

Acknowledgments

This work was supported by the RFBR grant 12-02-91504-CERN-a and the RAS-CERN program.

References

- [1] U. Amaldi, Small-angle physics at the intersecting storage rings forty years later, e-print arXiv:1206.3954, 2012.
- [2] U. Amaldi, K. Schubert, Impact parameter interpretation of proton-proton scattering from a critical review of all ISR data, Nuclear Physics B 166 (1980) 301 – 320.

²This curve differs slightly from that of [2] because we did not use the interpolation procedure adopted there but subtracted directly two overlap functions at 62.5 GeV and 23.5 GeV.

- [3] I.V. Andreev, I.M. Dremin, Large-angle elastic scattering, JETP Lett. 6 (1967) 262.
- [4] G. Antchev et al., Luminosity-independent measurements of total, elastic and inelastic cross-sections at root $s=7$ TeV, EPL 101 (2013) 21004.
- [5] G. Antchev et al., Measurement of proton-proton inelastic scattering cross-section at root $s=7$ TeV, EPL 101 (2013) 21003.
- [6] C. Bourrely, J.M. Myers, J. Soffer, T.T. Wu, High-energy asymptotic behavior of the bourrely-soffer-wu model for elastic scattering, Phys. Rev. D 85 (2012) 096009.
- [7] S. Chatrchyan et al., Jet and underlying event properties as a function of particle multiplicity in proton-proton collisions at $\sqrt{s} = 7$ TeV, FSQ-12-022, 2013.
- [8] I. Dremin, The black disk to be observed in the Orear region, Nuclear Physics A 888 (2012) 1 – 6.
- [9] I. Dremin, V. Nechitailo, Testing scaling laws for the elastic scattering of protons, Physics Letters B 720 (2013) 177 – 180.
- [10] I.M. Dremin, Elastic scattering of hadrons, Physics-Uspexhi 56 (2013) 3.
- [11] I.M. Dremin, V.A. Nechitailo, Elastic pp -scattering at $\sqrt{s} = 7$ tev with the genuine orear regime and the dip, Phys. Rev. D 85 (2012) 074009.
- [12] D.A. Fagundes, E.G.S. Luna, M.J. Menon, A.A. Natale, Aspects of a dynamical gluon mass approach to elastic hadron scattering at LHC, Nuclear Physics A 886 (2012) 48–70.
- [13] M.L. Good, W.D. Walker, Coulomb dissociation of beam particles, Phys. Rev. 120 (1960) 1855–1856.
- [14] F.S. Henyey, R.H. Tuan, G. Kane, Impact parameter study of high energy elastic scattering, Nuclear Physics B 70 (1974) 445 – 460.
- [15] R. Henzi, P. Valin, The inelastic differential cross section in impact parameter space at ISR energies, Physics Letters B 48 (1974) 119 – 124.
- [16] A. Kaidalov, Diffractive production mechanisms, Physics Reports 50 (1979) 157 – 226.
- [17] A.K. Kohara, E. Ferreira, T. Kodama, Amplitudes and observables in pp elastic scattering at root $s=7$ TeV, European Physical Journal C 73 (2013) 2326.
- [18] A.K. Kohara, E. Ferreira, T. Kodama, Elastic $p(\bar{p})$ scattering amplitude at 1.8 TeV and determination of total cross section, Phys. Rev. D 87 (2013) 054024.
- [19] S. Munier, A. Staśto, A. Mueller, Impact parameter dependent S-matrix for dipoleproton scattering from diffractive meson electroproduction, Nuclear Physics B 603 (2001) 427 – 445.
- [20] E. Nagy, R. Orr, W. Schmidt-Parzefall, K. Winter, A. Brandt, F. Bsser, G. Flgge, F. Niebergall, P. Schumacher, H. Eichinger, K. Schubert, J. Aubert, C. Broll, G. Coignet, H.D. Kerret, J. Favier, L. Massonnet, M. Vivargent, W. Bartl, H. Dibon, C. Gottfried, G. Neuhofer, M. Regler, Measurements of elastic proton-proton scattering at large momentum transfer at the CERN intersecting storage rings, Nuclear Physics B 150 (1979) 221 – 267.
- [21] K. Osterberg, talk at EPS-HEP 2013 conference, Stockholm, 2013.